# On the Equivalence of Hybrid Beamforming to Full Digital Zero Forcing in mmWave MIMO

Mohamed Shehata, Ali Mokh, Matthieu Crussière, Maryline Hélard, Patrice Pajusco

# On the Equivalence of Hybrid Beamforming to Full Digital Zero Forcing in mmWave MIMO

Mohamed Shehata[1], Ali Mokh[1], Matthieu Crussière[1], Maryline Hélard[1] and P. Pajusco[2]

[1]Univ Rennes, INSA Rennes, CNRS, IETR-UMR 6164, F-35000 Rennes
[2]Institut Mines-Telecom, Telecom Bretagne, CNRS UMR 6285 Lab-STICC, Brest, France

***Abstract*—Recently, Millimeter Wave (mmWave) systems have emerged as a potential solution for the spectrum secrecy problem suffered by current wireless technologies. However, practically implementing such systems is challenging as they suffer from high hardware complexity and power consumption. Therefore, analog beamforming is considered the most suitable approach for practical implementation of such systems, relaxing the hardware and power consumption requirements compared to full digital beamforming solution. Moreover, hybrid beamforming solutions emerged as an attractive solution that can capture the trade-off between digital and analog ones. In this paper we show mathematically that in pure Line of Sight (LoS) channels, using hybrid beamforming with Zero Forcing (ZF) at the baseband can achieve equivalent Spectral Efficiency (SE) compared to the full digital ZF precoding, with lower hardware complexity, and lower power consumption. Moreover, we validate the equivalence in SE performance between hybrid ZF and digital ZF by simulation results.**

***Index Terms*—Millimeter Wave (mmWave), Hybrid Beamforming, Multi user MIMO, Zero Forcing (ZF)**

## I. Introduction

The growing demand for higher achievable data rates and Energy Efficiency (EE) imposes a lot of challenges for the fifth generation of mobile networks [1]. In order to satisfy such demands the combination of Millimeter Wave (mmWave) systems and Massive MIMO became mandatory. Unleashing the high antenna array gains of Massive MIMO together with the high band-width at mmWaves, the data rates and EE can be enhanced significantly [2] [3].

However, achieving such gains of mmWave Massive MIMO systems is not straightforward, and opposed by many challenges. The most significant challenges can be summarized as follows:

- Hardware Complexity: In order to unleash the full gains of massive MIMO a dedicated Radio Frequency (RF) chain and mixed analog digital device are needed per antenna element in order to apply digital beamforming. Moreover, these elements are expensive and complex in mmWave frequencies [4].
- Power Consumption: Again, in order to apply digital beamforming at massive MIMO a lot of hardware components need to be installed at the transmitter and the receiver as aforementioned. Moreover, RF chains and mixed analog digital devices are power hungry at mmWave frequencies compared to microwave ones [5].
- Propagation Channel: At high frequencies the propagation channel is sparse and Line of Sight (LoS) dominated [6]. This, results in high path-loss, high sensitivity to blockage and tendency for high spatial correlation between closely spaced User Terminals (UTs)[7].

Motivated by the aforementioned challenges, analog beamforming has been proposed as a practical solution for mmWave massive MIMO systems. Utilizing the massive array gain of massive MIMO to overcome the severe path loss suffered by the mmWave propagation channel, analog beamforming was proposed as potential candidate for mmWave systems. In this case the link budget was considered more important compared to the SE gain offered by full digital beamforming (since the spectrum is not scarce anymore in mmWave frequenciess). Also, analog beamforming has low hardware and power consumption requirements (only one RF chain and mixed analog digital device is needed per transmitter/receiver), therefore favourable in terms of hardware complexity and power consumption compared to digital beamforming [8], [9].

However, recently Hybrid Beamforming (HBF) has emerged as a potential candidate for mmWave massive MIMO systems through striking a trade-off between digital and analog beamforming techniques. HBF can offer a flexible choice of the number of RF chains, therefore, leveraging a part of the multiplexing gain offered by digital beamforming and allowing for Multi User (MU) MIMO scenarios. Moreover, given the fact that in HBF the number of RF chains and mixed analog digital devices is much lower compared to the number of transmit/receive antennas, HBF is considered a hardware and power efficient beamforming solution [10]–[12].

Recent work in the literature [11], [12] showed that the SE performance gap between digital beamforming and HBF is minimal with small number of RF chains used in massive MIMO transmitters/receivers. This is due to the fact that mmWave channels are sparse, henceforth a few RF chains can be enough for having full access to the channel dominant paths. Moreover, in [13]–[15], it was shown that HBF can achieve the same SE as digital beamforming in case one of these conditions is met:

- In wide band system with analog network consisting of phase shifters together with variable gain amplifiers: if the number of RF chains is not smaller than $\min(N_{BS}, N_{S,sub})$, where $N_{BS}$ is the number of antennas at the Base Station (BS) and $N_{S,sub}$) is the total

number of data streams over all sub-carriers [13], [14].

- In wide band system with analog network consisting of phase shifters only: if $R$ RF chains are used and $2R(N_{BS} - R + 1)$ phase shifters are used, where $R \leq N_{BS}$ is the rank of the combined digital precoder matrices of all sub-carriers [15].
- In narrow band system with analog network consisting of phase shifters together with variable gain amplifiers: if the number of data streams $N_S$ is less than or equal the number of RF chains $N_{RF}$ ($N_S \leq N_{RF}$) [13], [14].
- In narrow band system with analog network consisting of phase shifters only: if the number of Rf chains is greater than or equal double the number of the data streams $N_{RF} \geq 2N_S$ [13], [14].

In this paper, we show that for HBF based on Zero Forcing (ZF) digital layer and an analog beamforming network of phase shifters only; it can achieve the same SE performance of the digital beamforming in pure LoS channels with only $N_{RF} \geq N_S$ in narrowband instead of the $N_{RF} \geq 2N_S$ in the literature. This can be achieved through adjusting the phases in the analog domain as will be shown later in details. Therefore, this paper can be considered considerable asset for the hardware and energy efficiency application of ZF in highly LoS channels. Throughout the paper, we provide mathematical analysis for our proposition and validate them with simulation results.

## II. System and Channel Model

In this paper we consider a narrowband downlink channel scenario, where the BS is equipped with multiple transmit antennas $N_{BS}$ serving $K$ UTs each equipped with a single receive antenna. Henceforth, the system tackled in this paper is a downlink MU Multiple Input Single Output (MISO) - Orthogonal Frequency Division Multiplexing (OFDM). The $N_{BS}$ antennas are deployed in a Uniform Linear Array (ULA) architecture. At the transmitter (BS) side the beamforming is applied, while at the receiver side (UT) no combining is applied as it has only a single receive antenna, and is limited to be served by a single stream.

The streams received by the $K$ UTs $\mathbf{r} = [R_1, R_2, ..., R_K]^T \in \mathbb{C}^{K\times 1}$ can be denoted as follows:

$$\mathbf{r} = \mathbf{H}\mathbf{x} + \mathbf{n} \tag{1}$$

where the independent and identically distributed (i.i.d.) Additive White Gaussian Noise(AWGN) vector is expressed as $\mathbf{n} = [N_1, N_2, ..., N_K]^T \in \mathbb{C}^{K\times 1}$ such that $n \sim \mathcal{N}(0, \sigma^2)$, and $\sigma^2$ is the noise variance. The MU MIMO channel matrix between the the $N_{BS}$ transmit antennas and the $K$ single receive antenna UTs is denoted as $\mathbf{H} \in \mathbb{C}^{K\times N_{BS}}$. Finally, $\mathbf{x} = [X_1, X_2, ..., X_{N_{BS}}]^T \in \mathbb{C}^{N_{BS}\times 1}$ is a vector that denotes the transmitted symbols at the BS after applying the beamforming and is expressed as:

$$\mathbf{x} = \mathbf{F}\mathbf{s} \tag{2}$$

where $\mathbf{F} = [\mathbf{f}_1, \mathbf{f}_2, ..., \mathbf{f}_K]^T$ is the beamforming matrix which can be fully digital or hybrid and will be described later. Finally, the vector of the transmitted symbols before beamforming is represented as $\mathbf{s} = [S_1, S_2, ..., S_K]^T \in \mathbb{C}^{K\times 1}$.

In this paper we utilize the sparse channel model adopted in most of the mmWave MIMO literature [12], [16]. This model abstracts the channel by a limited number of scatterers. Moreover, in this model each scatterer (cluster) is assumed to contribute by a single propagation ray. Therefore, for each UT $k$, the propagation channel vector $\mathbf{h}_k$ can be represented as:

$$\mathbf{h}_k = \sqrt{\frac{N_{BS}}{P_k}} \sum_{p=1}^{P_k} \alpha_{k,p} \mathbf{a}_t^H(\phi_{k,p}) \tag{3}$$

where $\alpha_{k,p}$ denotes the complex amplitude of the $p^{th}$ propagation path for UT $k$, given that $P_k$ represents the total number of paths for UT $k$. The channel complex values $\alpha$ are independent and identically distributed (i.i.d) complex Gaussian $\alpha \sim \mathcal{CN}(0, 1)$. $\phi_{k,p}$ represents the Angle of Departure (AoD) for each path $p$ for UT $k$ and is assumed to be uniformly distributed in the interval $[0, 2\pi]$.

$\mathbf{a}_t(\phi_{k,p})$ denotes the transmit array steering vector, since we deploy ULA array at the BS, the steering vector $\mathbf{a}_t(\phi_{k,p})$ is expressed as:

$$\mathbf{a}_t(\phi_{k,p}) = \frac{1}{\sqrt{N_{BS}}}[1, e^{j\zeta(\phi_{k,p})}, ..., e^{j(N_{BS}-1)\zeta(\phi_{k,p})}]^T \tag{4}$$

such that $\zeta(\phi_{k,p})$ is expressed as:

$$\zeta(\phi_{k,p}) = \frac{2\pi}{\lambda} d \sin(\phi_{k,p}) \tag{5}$$

where $\lambda$ is the signal's wavelength and $d$ denotes the inter-element antenna spacing. The MU channel matrix $\mathbf{H} \in \mathbb{C}^{K\times N_{BS}}$ is expressed as

$$\mathbf{H} = [\mathbf{h}_1^T, \mathbf{h}_2^T, ..., \mathbf{h}_K^T]^T \tag{6}$$

In this paper, we consider a pure LoS scenario ($P_k = 1, \forall K$), which is a fairly acceptable assumption for mmWave channels at high frequences. This consideration is taken, since in this case the HBF with ZF can achieve the same SE as digital beamforming for narrowband systems with phase shifters only in the analog domain. This can be achieved given some phase adjustments in the analog domain under the condition $N_{RF} \geq N_S$ instead of $N_{RF} \geq 2N_S$ in the literature [14], [17]. Therefore, substituting $P_k = 1$ in Equation (3), the pure LoS channel for each UT $k$ can be expressed as:

$$\mathbf{h}_k = \sqrt{N_{BS}}\ \alpha_k \mathbf{a}_t^H(\phi_k) \tag{7}$$

## III. Beamforming Scenarios

In this section the beamforming strategies adopted in the paper, which are the fully digital ZF, the hybrid ZF and the analog LoS beamsteering, are detailed. Moreover, we show by mathematical analysis how both hybrid ZF and fully digital one achieve the same SE when the phases of HBF are efficiently manipulated using the LoS beamsteering in the analog domain.

### A. Analog Beamsteering for LoS Channel

This approach is the most classic analog beamforming, specifically for LoS dominant environments such as mmWave environments [12]. In this approach the analog beam is steered towards the channel path with the highest power (LoS path).

Thus, the knowledge of the LoS AoD $\phi_{k,p_{LoS}}$ is only required for calculating the LoS beamsteering vector as follows:

$$\mathbf{f}_{LoS} = \mathbf{a}_t(\phi_{p_{LoS}}) \tag{8}$$

### B. Hybrid Beamforming

Here the hybrid beamforming architecture is introduced in order to extend the previously proposed analog beamforming algorithm for multiplexing and SE gains. Throughout the paper, the RF and Base Band (BB) architectures are decoupled as in [12]. Then the equivalent channel for each UT $k$, $\hat{\mathbf{h}}_k$ is formed before the digital processing layer as follows:

$$\hat{\mathbf{h}}_k = \mathbf{h}_k \mathbf{F}_{RF}, \tag{9}$$

such that, $\mathbf{h}_k \in \mathbb{C}^{1\times N_{BS}}, \hat{\mathbf{h}}_k \in \mathbb{C}^{1\times N_{RF}}$ and $\mathbf{F}_{RF} \in \mathbb{C}^{N_{BS}\times N_{RF}}$ represents the analog beamforming matrix and is computed as:

$$\mathbf{F}_{RF} = [\mathbf{f}_{RF,1}, ..., \mathbf{f}_{RF,K}] \tag{10}$$

such that $\mathbf{f}_{RF,k}$ is the analog beamforming vector for UT $k$ and is chosen throughout this paper as the LoS beamsteering analog beamformer as follows: $\mathbf{f}_{RF,k} = \mathbf{f}_{LoS,k}$.

Then the total virtual channel for the $K$ UTs $\hat{\mathbf{H}}$ is represented as:

$$\hat{\mathbf{H}} = [\hat{\mathbf{h}}_1^T, ..., \hat{\mathbf{h}}_K^T] \tag{11}$$

Finally, we utilize the ZF digital precoding to suppress the inter-user interference. Hence, the digital beamformer is calculated as follows:

$$\mathbf{W} = \hat{\mathbf{H}}^H(\hat{\mathbf{H}}\hat{\mathbf{H}}^H)^{-1} \tag{12}$$

Then, the digital beamformer is normalized to satisfy the total power constraint. As illustrated in the literature [18], [19], ZF can be normalized using two different methods namely Vector Normalization (VN) and Matrix Normalization (MN). It is shown in [19], that VN has always superior performance over MN in terms of SE. Therefore, throughout the paper we will use VN for ZF normalization in HBF and full digital beamforming. Therefore applying the VN on the digital beamforming part $\mathbf{W}$ of the hybrid beamformer $\mathbf{F}^{HBF}$, then the per stream digital beamformer $\mathbf{w}_k$ for each UT $k$ is expressed as follows:

$$\mathbf{w}_k = \frac{\mathbf{w}_k}{\|\mathbf{f}_k^{HBF}\|} = \frac{\mathbf{w}_k}{\|\mathbf{F}_{RF}\mathbf{w}_k\|} \tag{13}$$

where $\mathbf{f}_k^{HBF}$ is the hybrid beamforming vector for UT $k$. The calculation of the hybrid beamformer $\mathbf{F}^{HBF} = \mathbf{F}_{RF}\mathbf{W}$ is summarized in Algorithm (1).

**Algorithm 1** Two Stage Decoupled RSM Hybrid Beamforming

1) **Fisrt Stage:** RF Analog Beamforming **such that**
$$\mathbf{F}_{RF} = [\mathbf{f}_{RF,1}, ..., \mathbf{f}_{RF,K}]$$
$\mathbf{f}_{RF,k}$ is chosen as $\mathbf{f}_{LoS,k}$
2) Calculate the equivalent channel $\hat{\mathbf{H}}$ as:
$$\hat{\mathbf{H}} = [\hat{\mathbf{h}}_1^T, ..., \hat{\mathbf{h}}_K^T]$$
$\hat{\mathbf{h}}_k = \mathbf{h}_k\mathbf{F}_{RF}, (\mathbf{h}_k \in \mathbb{C}^{1\times N_{BS}}, \mathbf{F}_{RF} \in \mathbb{C}^{N_{BS}\times N_{RF}}, \hat{\mathbf{h}}_k \in \mathbb{C}^{1\times N_{RF}})$
3) **Second Stage:** Digital Precoding such that
$\mathbf{W}$ can be chosen as any Base Band (BB) technique. Here we choose ZF, hence $\mathbf{W} = \mathbf{W}_{ZF}$
4) Here the digital beamforming $\mathbf{W}$ is applied on the equivalent channel $\mathbf{H}_e$ instead of the propagation channel $\mathbf{H}$. Hence, replacing $\mathbf{H}$ by $\mathbf{H}_e$, the beamformer is calculated as:
$$\mathbf{W}_{ZF} = \mathbf{H}_e^H(\mathbf{H}_e\mathbf{H}_e^H)^{-1}$$
5) The digital beamformer column vectors are normalized to satisfy the total power constraint as follows $\mathbf{w}_k = \frac{\mathbf{w}_k}{\|\mathbf{F}_{RF}\mathbf{w}_k\|}$
6) Finally the hybrid beamformer is calculated as:
$$\mathbf{F}^{HBF} = \mathbf{F}_{RF}\mathbf{W}_{ZF}$$

### C. Digital Beamforming

In this case the digital beamforming ZF matrix $\mathbf{F}^{ZF}$ is calculated directly from the propagation channel $\mathbf{H} \in \mathbb{C}^{K\times N_{BS}}$ as follows:

$$\mathbf{F}^{ZF} = \mathbf{H}^H(\mathbf{H}\mathbf{H}^H)^{-1} \tag{14}$$

Then, VN is applied per beamforming vector $\mathbf{f}_k^{ZF}$ as follows:

$$\mathbf{f}_k^{ZF} = \frac{\mathbf{f}_k^{ZF}}{\|\mathbf{f}_k^{ZF}\|} \tag{15}$$

### D. Spectral Efficiency Analysis

The instantaneous per stream $SE_k$ is well known to be expressed as follows:

$$\text{SE}_k = \log_2(1 + \text{SINR}_k) \tag{16}$$

given the fact that the instantaneous Signal to Interference and Noise Ratio (SINR) for UT $k$ in case fully digital ZF beamforming is applied, is expressed as follows [7], [19]:

$$\text{SINR}_k^{ZF} = \frac{\beta}{\|\mathbf{f}_k^{ZF}\|^2} \tag{17}$$

where $\beta$ is the transmit Signal to Noise Ratio (SNR). According to ([19]), $\|\mathbf{f}_k^{ZF}\|^2$ can be represented as:

$$\|\mathbf{f}_k^{ZF}\|^2 = ((\mathbf{H}\mathbf{H}^H)^{-1})_{k,k} \tag{18}$$

substituting Equation (18) in (17), then $\text{SINR}_k^{ZF}$ is expressed as

$$\text{SINR}_k^{ZF} = \frac{\beta}{((\mathbf{H}\mathbf{H}^H)^{-1})_{k,k}} \tag{19}$$

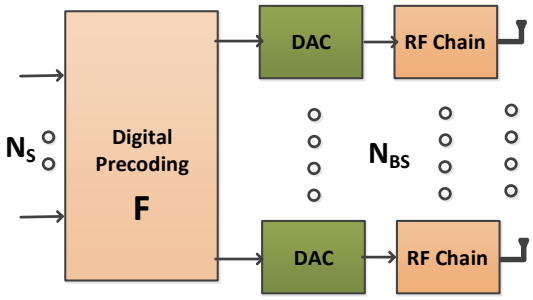


Figure 1: The fully digital beamforming architecture.

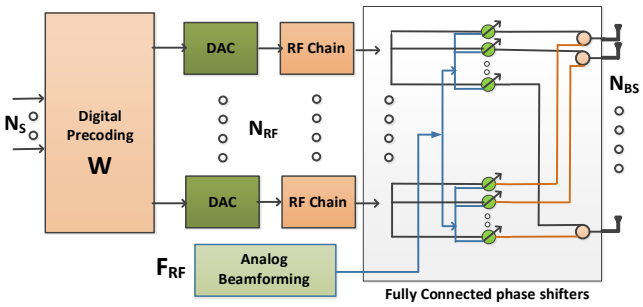


Figure 2: The fully connected HBF architecture.

Similarly, in case HBF with ZF digital layer is applied, the SINR for UT $k$ is expressed as follows:

$$\text{SINR}_k^{HBF} = \frac{\beta}{\|\mathbf{f}_k^{HBF}\|^2} \tag{20}$$

where $\|\mathbf{f}_k^{HBF}\|^2$ can be expressed as:

$$\|\mathbf{f}_k^{HBF}\|^2 = \|\mathbf{F}_{RF}\mathbf{w}_k\|^2 = (\mathbf{F}_{RF}\mathbf{w}_k)^H(\mathbf{F}_{RF}\mathbf{w}_k) \tag{21}$$

since $(\mathbf{F}_{RF}\mathbf{W})^H$ can be expressed as

$$\begin{aligned}(\mathbf{F}_{RF}\mathbf{W})^H &= (\mathbf{F}_{RF}^H\mathbf{H}^H(\mathbf{H}\mathbf{F}_{RF}\mathbf{F}_{RF}^H\mathbf{H}^H)^{-1})^H\mathbf{F}_{RF}^H \\ &= ((\mathbf{H}\mathbf{F}_{RF})^{-1})^H\mathbf{F}_{RF}^H = (\mathbf{H}^H)^{-1}\end{aligned} \tag{22}$$

similarly $(\mathbf{F}_{RF}\mathbf{W})$ can be expressed as

$$\begin{aligned}(\mathbf{F}_{RF}\mathbf{W}) &= \mathbf{F}_{RF}\mathbf{F}_{RF}^H\mathbf{H}^H(\mathbf{H}\mathbf{F}_{RF}\mathbf{F}_{RF}^H\mathbf{H}^H)^{-1} \\ &= \mathbf{F}_{RF}(\mathbf{H}\mathbf{F}_{RF})^{-1} = (\mathbf{H})^{-1}\end{aligned} \tag{23}$$

From Equations (22) and (23), Equation (21) can be reformulated as follows:

$$\|\mathbf{f}_k^{HBF}\|^2 = ((\mathbf{H}^H)^{-1}(\mathbf{H})^{-1})_{k,k} = ((\mathbf{H}\mathbf{H}^H)^{-1})_{k,k} \tag{24}$$

substituting Equation (24) in (20), then $\text{SINR}_k^{HBF}$ is expressed as

$$\text{SINR}_k^{HBF} = \frac{\beta}{((\mathbf{H}\mathbf{H}^H)^{-1})_{k,k}} \tag{25}$$

Therefore from Equations (19) and (25) we prove that both fully digital ZF and HBF based on ZF achieve the same SE in pure LoS channels. This is valid as long the the number of RF chains is at least equal to the number of data streams $N_S$. Hence achieving the same SE of ZF digital beamforming with massive complexity and power consumption reduction. In this paper the total number of data streams $N_S$ is equal to the number of UTs $K$, since each UT has a single receive antenna and thus served by a single stream.

## IV. Hardware and Power Consumption Model

In this section, we describe the hardware architecture of the two systems introduced in this paper with are the fully digital ZF and the HBF ZF. Moreover, power realistic consumption models in [20] are used for both systems.

Table I: Hardware Complexity Comparison

| Component | Digital Beamforming | HBF |
|---|---|---|
| Power Amplifier | 1 | 1 |
| Phase Shifter | 0 | $N_{RF}N_{BS}$ |
| Local Oscillator | 1 | 1 |
| RF Chain | $N_{BS}$ | $N_{RF}$ |
| DAC | $N_{BS}$ | $N_{RF}$ |

### A. Hardware Architectures

As aforementioned in this paper, we consider two hardware architectures, namely the fully digital beamforming architecture illustrated in Figure 1 and the fully connected HBF illustrated in Figure 2.

Given the fact that both architectures achieve the same SE in case ZF is used in the digital layer (baseband) in pure LoS channels as previously proved, our aim here is to evaluate the hardware efficiency for both architectures. The hardware efficiency can be seen as the achieved SE relative to the number of hardware complex components needed. In our case, since both achieve the same SE, the hardware efficiency is inversely proportional to the number of complex components needed.

Therefore, from both Figures 1 and 2, the number of hardware elements for each architecture can be deduced. We summarize the hardware complexity for both architectures in Table I.

Given that in massive MIMO the number of transmit antennas $N_{BS}$ is much larger than the number of UTs $N_{BS} >> K$, and given that in our HBF we utilize RF chains equal to the number of data streams because we already proven that for $N_{RF} > N_S$ no further SE gain will be achieved compared to $N_{RF} = N_S$ in case ZF digital processing is applied in LoS channel. Also, in our case the number of streams $N_S$ is equal to the number of UTs $K$, since each UT is served by a single stream. Therefore, to sum up, in fully connected HBF architecture we have $N_{RF} = N_S = K << N_{BS}$ while in fully digital one we have $N_{RF} = N_{BS} >> K$. Henceforth, we can conclude that HBF is much more hardware efficient in our scenario due to the massive reduction in the number of required DACs and RF chains compared to the fully digital one.

Table II: Power Consumption of the Analog Components [20]

| Component | Value |
|---|---|
| Power Amplifier ($P_{PA}$) | $\frac{P_t}{\eta}, \eta = 27\%$ |
| Phase Shifter ($P_{PS}$) | for $b_{PS} = 4, 21.6$ mW |
| Local Oscillator ($P_{LO}$) | 22.5 mW |
| 90 deg hybrid with buffers ($P_H$) | 3 mW |
| Mixer ($P_M$) | 0.3 mW |
| Low Pass Filter ($P_{LP}$) | 14 mW |
| RF Chain ($P_{RF}$) | 31.6 mW |
| DAC ($P_{DAC}$) | Equation (28) |

### B. Power Consumption Models

First we start by defining the power consumption per RF chain $P_{RF}$ as follows:

$$P_{RF} = 2P_{LP} + 2P_M + P_H \tag{26}$$

where $P_{LP}$, $P_M$ and $P_H$ represent the power consumption by the low pass filter, the mixer, and the 90 deg hybrid respectively.

The power consumption for the full digital ZF can be defined as:

$$P_D = P_{LO} + P_{PA} + N_{BS}(2P_{DAC} + P_{RF}) \tag{27}$$

where $P_{LO}$ is is the power consumption of the local oscillator, $P_{PA}$ is the power consumption of the power amplifier which is calculated as $P_{PA} = \frac{P_t}{\eta}$ where $P_t$ is the transmit power and $\eta$ is the power amplifier efficiency. Finally $P_{DAC}$ is the power consumption at the Digital to Analog Converter (DAC) and is represented as:

$$P_{DAC} = 1.5(10^{-5})(2^{b_{DAC}}) + 9(10^{-12})(b_{DAC})(F_s) \tag{28}$$

where $b_{DAC}$ and $F_s$ denote the number of bits of resolution of the DAC and its sampling rate in Hertz respectively.

Moving the HBF architecture with fully connected phase shifters, the power consumption in this case is represented as:

$$P_{HBF} = P_{LO} + P_{PA} + N_{RF}(2P_{DAC} + P_{RF}) + N_{BS}N_{RF}P_{PS} \tag{29}$$

where $P_{PS}$ is the power consumed by the phase shifter and it depends on the number of resolution bits $b_{PS}$.

Typical values for all the aforementioned terms in mmWave regime are summarized in Table II according to [20].

## V. Simulation Results

In this section, we validate our SE analysis for both fully digital ZF and HBF based on ZF digital layer in pure LoS channel. Moreover, we compare between both architectures in terms of EE, together with the HBF architecture with the constraint $N_{RF} = 2N_S = 2K$ provided in the literature [13], [14]. The transmit antenna array is ULA with half wavelength spacing, and the number of transmit RF chains $N_{Rf}$ equals the number of transmit antennas in case of fully digital scenaro $N_{RF}^{ZF} = N_{BS}$, and equals to the number of UTs in our proposed HBF scenario $N_{RF}^{HBF,1} = K$. On the other hand, $N_{RF}^{HBF,2} = 2K$ characterizes the HBF architecture in [13], [14]. The simulations are done in Monte Carlo fashion with 1000 realizations. Finally, perfect Channel State Information at the Transmitter (CSIT) is assumed.

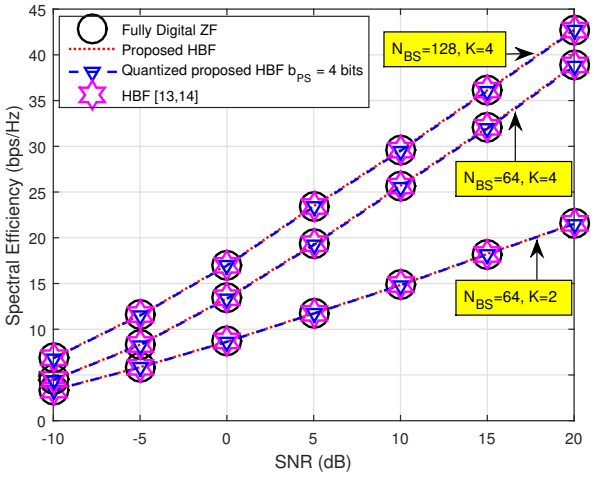


Figure 3: SE comparison for the proposed beamforming architectures for different $N_{BS}$ and $K$.

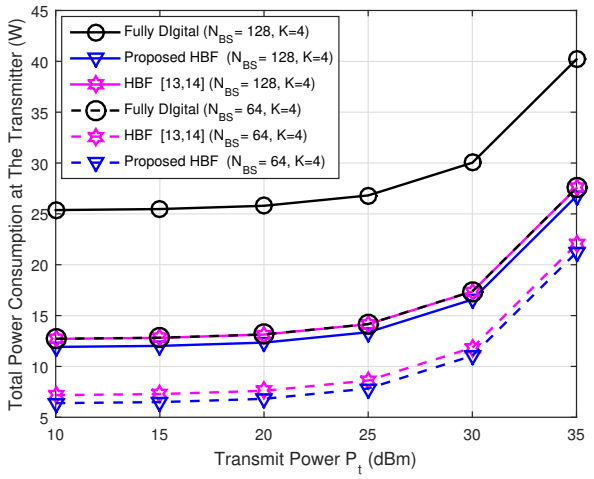


Figure 4: Transmitter power consumption comparison for the proposed beamforming architectures for different $N_{BS}$ and $K$.

In Figure 3 we validate our SE analysis by comparing the SE of the proposed HBF architecture that has the condition $N_{RF} = K$, with the fully digital architecture ($N_{RF} = N_{BS}$) and the HBF in [14], [17] that has the condition $N_{RF} = 2K$. We can observe that for different simulation setups (different $K$ and $N_{BS}$), all the beamforming architectures achieve exactly the same SE. Thus, highlighting the privilege of our proposed HBF architecture for ZF baseband processing in LoS channels. Moreover, in order to have realistic insights we

consider quantized phase shifters ($b_{PS}$). It is shown in Figure 3, that even with this coarse 4 bits phase quantization, the SE degradation is negligible compared to using infinite resolution phase shifters when the number of transmit antennas $N_{BS}$ is sufficiently high.

In Figure 4 we compare the total power consumption at the transmitter for all the introduced architectures as a measure of the EE. Since all the introduced architectures achieve the same SE, the EE can be directly seen as the inverse of the power consumption. We can observe that our proposed HBF architecture is the most energy efficient compared to the fully digital and HBF architecture proposed in [14].

## VI. Conclusion

In this paper, we provided a hardware, energy and spectral efficient hybrid beamforming architecture for zero forcing in LoS channels. We showed by mathematical analysis and validated with simulation results that using the proposed hybrid beamforming architecture can achieve the same SE as the fully digital ZF which requires high hardware complexity and power consumption in mmWave massive MIMO systems. Moreover, we relaxed the constraint of equity between hybrid beamforming and fully digital one in the literature to simply having number of RF chains equal to the number of data streams for our proposed scenario.

## VII. Acknowledgement

The authors would like to thank the SPATIAL MODULATION project funded by the French National Research Agency (ANR). Also, This work has received a French state support granted to the CominLabs excellence laboratory and managed by the National Research Agency in the Investing for the Future program under reference Nb. ANR-10-LABX-07-01 and project name M$^5$HESTIA (**mm**Wave **M**ulti-user **M**assive **M**IMO **H**ybrid **E**quipments for **S**ounding, **T**ransmissions and HW **I**mplement**A**tion).

## References

[1] J. F. Monserrat, H. Droste, O. Bulakci, J. Eichinger, O. Queseth, M. Stamatelatos, H. Tullberg, V. Venkatkumar, G. Zimmermann, U. Dötsch, and A. Osseiran, "Rethinking the mobile and wireless network architecture: The metis research into 5g," in *2014 European Conference on Networks and Communications (EuCNC)*, June 2014, pp. 1–5.

[2] E. G. Larsson, O. Edfors, F. Tufvesson, and T. L. Marzetta, "Massive mimo for next generation wireless systems," *IEEE Communications Magazine*, vol. 52, no. 2, pp. 186–195, February 2014.

[3] M. Xiao, S. Mumtaz, Y. Huang, L. Dai, Y. Li, M. Matthaiou, G. K. Karagiannidis, E. Björnson, K. Yang, C. I, and A. Ghosh, "Millimeter wave communications for future mobile networks," *IEEE Journal on Selected Areas in Communications*, vol. 35, no. 9, pp. 1909–1935, Sep. 2017.

[4] Z. Zhou, N. Ge, Z. Wang, and S. Chen, "Hardware-efficient hybrid precoding for millimeter wave systems with multi-feed reflectarrays," *IEEE Access*, vol. 6, pp. 6795–6806, 2018.

[5] R. Méndez-Rial, C. Rusu, N. González-Prelcic, A. Alkhateeb, and R. W. Heath, "Hybrid mimo architectures for millimeter wave communications: Phase shifters or switches?" *IEEE Access*, vol. 4, pp. 247–267, 2016.

[6] S. Rangan, T. S. Rappaport, and E. Erkip, "Millimeter-wave cellular wireless networks: Potentials and challenges," *Proceedings of the IEEE*, vol. 102, no. 3, pp. 366–385, March 2014.

[7] H. Tataria, P. J. Smith, L. J. Greenstein, P. A. Dmochowski, and M. Matthaiou, "Impact of line-of-sight and unequal spatial correlation on uplink mu-mimo systems," *IEEE Wireless Communications Letters*, vol. 6, no. 5, pp. 634–637, Oct 2017.

[8] Y. Zou, Q. Li, G. Yang, and X. Cheng, "Analog beamforming for millimeter-wave mimo systems via stochastic optimization," in *2016 8th International Conference on Wireless Communications Signal Processing (WCSP)*, Oct 2016, pp. 1–5.

[9] X. Li, Y. Zhu, and P. Xia, "Enhanced analog beamforming for single carrier millimeter wave mimo systems," *IEEE Transactions on Wireless Communications*, vol. 16, no. 7, pp. 4261–4274, July 2017.

[10] O. E. Ayach, S. Rajagopal, S. Abu-Surra, Z. Pi, and R. W. Heath, "Spatially sparse precoding in millimeter wave mimo systems," *IEEE Transactions on Wireless Communications*, vol. 13, no. 3, pp. 1499–1513, March 2014.

[11] A. Alkhateeb, O. E. Ayach, G. Leus, and R. W. Heath, "Channel estimation and hybrid precoding for millimeter wave cellular systems," *IEEE Journal of Selected Topics in Signal Processing*, vol. 8, no. 5, pp. 831–846, Oct 2014.

[12] A. Alkhateeb, G. Leus, and R. W. Heath, Jr, "Limited Feedback Hybrid Precoding for Multi-User Millimeter Wave Systems," *ArXiv e-prints*, Sep. 2014.

[13] A. F. Molisch, V. V. Ratnam, S. Han, Z. Li, S. L. H. Nguyen, L. Li, and K. Haneda, "Hybrid beamforming for massive mimo: A survey," *IEEE Communications Magazine*, vol. 55, no. 9, pp. 134–141, Sep. 2017.

[14] X. Zhang, A. F. Molisch, and S.-Y. Kung, "Variable-phase-shift-based rf-baseband codesign for mimo antenna selection," *IEEE Transactions on Signal Processing*, vol. 53, no. 11, pp. 4091–4103, Nov 2005.

[15] T. E. Bogale, L. B. Le, A. Haghighat, and L. Vandendorpe, "On the number of rf chains and phase shifters, and scheduling design with hybrid analog–digital beamforming," *IEEE Transactions on Wireless Communications*, vol. 15, no. 5, pp. 3311–3326, May 2016.

[16] A. M. Sayeed, "Deconstructing multiantenna fading channels," *IEEE Transactions on Signal Processing*, vol. 50, no. 10, pp. 2563–2579, Oct 2002.

[17] A. F. Molisch, V. V. Ratnam, S. Han, Z. Li, S. L. H. Nguyen, L. Li, and K. Haneda, "Hybrid beamforming for massive mimo: A survey," *IEEE Communications Magazine*, vol. 55, no. 9, pp. 134–141, 2017.

[18] M. Sadeghi, L. Sanguinetti, R. Couillet, and C. Yuen, "Large system analysis of power normalization techniques in massive mimo," *IEEE Transactions on Vehicular Technology*, vol. 66, no. 10, pp. 9005–9017, Oct 2017.

[19] Y. Lim, C. Chae, and G. Caire, "Performance analysis of massive mimo for cell-boundary users," *IEEE Transactions on Wireless Communications*, vol. 14, no. 12, pp. 6827–6842, Dec 2015.

[20] L. N. Ribeiro, S. Schwarz, M. Rupp, and A. L. F. de Almeida, "Energy efficiency of mmwave massive mimo precoding with low-resolution dacs," *IEEE Journal of Selected Topics in Signal Processing*, vol. 12, no. 2, pp. 298–312, May 2018.